Spontaneous emission in a coupled cavity array featuring random-dimer disorder

Mariana O. Monteiro,[1] Guilherme M. A. Almeida,[1] and Francisco A. B. F. de Moura[1]

[1]*Instituto de Física, Universidade Federal de Alagoas, 57072-900 Maceió, AL, Brazil*

Abstract

We study the emission dynamics of a two-level atom interacting with a large array of coupled cavities via the central site. The local frequencies of the cavities follow a random dimer model, where two distinct frequency values are sorted across the array, with one value occurring only between pairs of adjacent sites. This configuration results in the coexistence of localized and quasi-extended field modes, which we exploit to measure the Markovian character of the amplitude-damping channel. By tuning the correlation length of the disorder, we observe a transition from non-Markovian to Markovian decay at specific values of the atomic frequency. In this setup, the atom serves as a probe for the localization properties of the array, establishing a connection between the theory of open quantum systems and quantum transport in low-dimensional systems.

I. INTRODUCTION

The development of large-scale fault-tolerant quantum computers is challenging due to the detrimental effects of decoherence [1, 2]. Qubits are susceptible to interactions with their surrounding environment, making it crucial to devise effective strategies for controlling quantum dynamics. One approach is to tailor the environment to achieve the desired open system dynamics in a more controlled setting [3–6]. These so-called structured environments – possessing nontrivial spectral densities – have proven to be powerful tools in advancing quantum technologies, such as enabling the creation of exotic quantum states [7, 8], aiding quantum simulation of open quantum systems [9–11], and more [12, 13].

Considering the problem of spontaneous emission of a two-level atom, a variety of structured environments inspired by photonic crystals have been explored [14]. The emission dynamics obeys the mode structure of the electromagnetic field with which the atom interacts. Two paradigmatic dynamical regimes are: (i) the memoryless and irreversible decay of the atomic population, when such environment is characterized by a flat spectral density (as the decay in open space) and (ii) vacuum Rabi oscillations when the atomic frequency is in resonance with a field mode having an extremely narrow lineshape. Often, when the environment is assumed to be described by a smooth spectral density (say, a flat one), a Lindblad master equation can be derived under the Born-Markov approximations. From the broader perspective of quantum dissipation theory, this means the local action of the environment is given by a quantum dynamical semigroup of complete positive trace-preserving

maps [15]. The underlying geometry of photonic crystals along with the likely occurrence of defects and disorder [16, 17] will, in contrast, lead to singularities and band gaps in the density of states, thereby rendering non-Markovian dynamics [14]. Physically, this means that information can flow back into the system [4, 10, 11, 18–32] as the emitted field retains memory.

The phenomenon addressed above raises the idea of exploring distinct non-Markovian behavior arising from the transport properties of low-dimensional systems [4, 33–36]. An important result in this direction was obtained by Lorenzo *et al.* [4], who reported emergent non-Markovian behavior in the emission of an atom weakly interacting with a coupled-cavity array (CCA) undergoing Anderson localization of the field modes. A homogeneous CCA, in contrast, lead to Markovian (memoryless) exponential decay of the excitation due to the flat spectral density structure in the center of the band. Recently, in the same setting, a localization-delocalization transition driven by long-range correlated disorder was investigated, revealing a transition from non-Markovian to Markovian behavior [37]. This connection between quantum optics and condensed-matter physics is appealing, especially in the context of the Noisy Intermediate-Scale Quantum era [38]. On one hand, non-trivial lattice configurations can be used to control non-Markovian dynamics. On the other, the dynamics of a small subsystem (the atom) can be analyzed to probe the spectral properties of the environment [39–42]. Quantum probing schemes based on dissipative dynamics can thus be used to access complex many-body phenomena such as quantum phase transitions [4, 43–46], as well as anomalous transport properties supported by correlated disorder [37]. Unlike standard Anderson localization theory, which predicts that any amount of disorder in 1D and 2D lattices leads to exponential localization of all modes [47], statistical correlations embedded in the disorder provide a route to evade it [48].

In this work, we further explore the relationship between non-Markovianity and quantum transport by exploring the emission dynamics of a single atom embedded in a CCA whose local frequencies feature short-range correlated defects. Our configuration is rooted in the idea of random-dimer disorder [49], which allows the occurrence of extended states within the allowed energy band despite the lack of homogeneity. This was first experimentally confirmed in [50], where the authors reported that short-range spatial correlations in GaAs-AlGaAs superlattices inhibited localization. In Ref. [51], a transition between ballistic and superdiffusive expansion was observed in a 1D array of weakly coupled waveguides directly

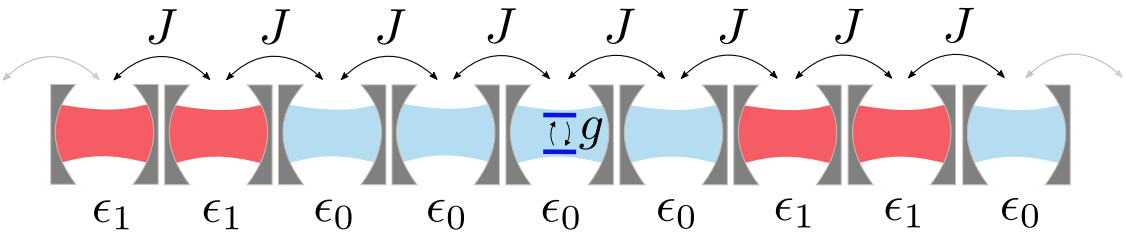

FIG. 1. Sketch of an array of single-mode optical cavities coupled at tunneling rate J. A single two-level atom (a qubit) is confined at the center cavity and coupled with its field mode at rate g undergoing a Jaynes-Cummings type interaction. Short-range correlated disorder is introduced as random defects in the field frequency distribution occurring in adjacent pairs assuming ϵ_1. The remaining cavities are set to frequency $\epsilon_0 \equiv 0$.

written in fused silica. This setup consisted of two types of propagation constants, one of which appeared in pairs. More recently, a metal-insulator transition was observed in a topological Si_3N_4 waveguide array [52]. These results illustrate that random-dimer disorder remains a relevant tool to explore non-trivial aspects of quantum transport properties in low-dimensional systems [53] and is within current experimental capabilities.

Our CCA featuring random-dimer disorder is shown in Fig. 1. This disorder introduces spatial correlations in the cavity frequencies through defects of the same frequency ϵ_1 randomly assigned to pairs of adjacent cavities along the CCA, leaving ϵ_0 otherwise. Here, we revisit key localization properties of the random-dimer model in association with the memory effects occurring during the dissipation dynamics of the atom. By means of a non-Markovinanity measure that tracks the amount of excitation backflow into the atom [4, 37], we observe a transition from non-Markovian to Markovian (memoryless) decay regimes arising from the resonance between the atomic frequency and the defect frequency ϵ_1. At this level, the emission dynamics becomes strongly influenced by extended field normal modes, effectively rendering a flat spectral density [14]. Our findings highlight the use of correlated disorder profiles, such as those based on the random dimer model, as a versatile platform for controlling quantum dissipation.

II. MODEL

Let us consider a CCA described by the Hamiltonian $\hat{H} = \hat{H}_0 + \hat{H}_I$, where ($\hbar = 1$)

$$\hat{H}_0 = \sum_{i=-N/2}^{N/2} \left[\epsilon_i \hat{a}_i^\dagger \hat{a}_i + J(\hat{a}_i \hat{a}_{i+1}^\dagger + \hat{a}_i^\dagger \hat{a}_{n+1}) \right], \tag{1}$$

$$\hat{H}_I = \omega_a \hat{\sigma}_+ \hat{\sigma}_- + g(\hat{\sigma}_+ \hat{a}_0 + \hat{\sigma}_- \hat{a}_0^\dagger), \tag{2}$$

with $\hat{a}_i$ ($\hat{a}_i^\dagger$) being the annihilation (creation) operator acting at the ith cavity, ϵ_i the local cavity frequency, ω_a the atomic transition frequency, and σ_+ (σ_-) the atomic raising (lowering) operator. The first term $\hat{H}_0$ accounts for the free-field part of the Hamiltonian, which describes photon tunneling at rate J through the $N+1$ cavities (we take N even without loss of generality). As this hopping parameter is homogeneous across the array, hereafter we set $J \equiv 1$ as the standard frequency unit. The interaction part $\hat{H}_I$ represents the Jaynes-Cummings interaction between the atom and the central cavity at rate g, which we will fix to $g = 0.1$ throughout. This embodies the weak-coupling regime that, in a homogeneous CCA, leads to exponential (Markovian) decay of the atomic population $\sim e^{-g^2 t/J}$ [4, 34].

Indeed, to grasp how the CCA functions as an environment, let us rewrite the full Hamiltonian in terms of the interaction between the atom and the field normal modes $\hat{\phi_k}^\dagger = |\phi_k\rangle\langle \text{vac}|$, where $\hat{H}_0|\phi_k\rangle = E_k|\phi_k\rangle$ and E_k are the corresponding eigenvalues (frequencies). We then obtain

$$\hat{H} = \omega_a \hat{\sigma}_+ \hat{\sigma}_- + \sum_k E_k \hat{\phi_k}^\dagger \hat{\phi_k} + \sum_k g_k (\hat{\phi_k} \hat{\sigma}_+ + \hat{\phi_k}^\dagger \hat{\sigma}_-), \tag{3}$$

with the effective coupling $g_k \equiv g\langle 0|\phi_k\rangle$ being the component of the field normal mode at the cavity that contains the atom. The Hamiltonian above represents the standard framework for dealing with open two-level quantum systems, where the environment is made up by a collection of bosonic modes. [15].

The spontaneous emission of the atom is investigated by means of the time evolution of the state $|\psi(t=0)\rangle = |e\rangle|\text{vac}\rangle$, that is the excited atom with the field vacuum. As the CCA Hamiltonian commutes with the total number of excitations, the dynamics takes place in the single-excitation manifold $\{|e\rangle|\text{vac}\rangle, \{|g\rangle|\phi_k\rangle\}\}$, where $|g\rangle$ denotes the atomic ground state. The evolved state is obtained via $|\psi(t)\rangle = \hat{U}|\psi(t=0)\rangle$, where $\hat{U} = e^{-i\hat{H}t}$ is the unitary

quantum time evolution operator. At an arbitrary time t, the state reads

$$|\psi(t)\rangle = f_e(t)|e\rangle|\text{vac}\rangle + \sum_k f_k(t)|g\rangle|\phi_k\rangle, \tag{4}$$

where $f_e(t)$ and $f_k(t)$ are the corresponding time-dependent amplitudes, which obey:

$$\dot{f}_e(t) = -i\omega_a f_e(t) - i\sum_k g_k f_k(t), \tag{5}$$

$$\dot{f}_k(t) = -iE_k f_k(t) - ig_k f_a(t). \tag{6}$$

Manipulating both equations above, an integro-differential equation for $f_e(t)$ is obtained in the form

$$\dot{f}_e(t) = -i\omega_a f_e(t) - \int_0^t \sum_k g_k^2 e^{-iE_k(t-t')} f_e(t')dt'. \tag{7}$$

Note that for a continuum spectrum, one can proceed by replacing $\sum_k g_k^2 \to \int G(E)dE$, with $G(E)$ being the spectral density of the CCA environment, which encapsulates all the essential details about its interaction with the atom.

In the absence of any kind of disorder, the CCA embodies a flat spectral density, $G(E) = const$, assuming a weak atom-field interaction $g \ll J$ and given the smooth dispersion profile in the center of the Bloch band. As such, the CCA effectively behaves as a Markovian environment leading to the exponential decay of the atom [34] as if it were in open space [14]. A non-homogeneous CCA, on the other hand, renders non-trivial spectral densities and therefore non-Markovian behavior is obtained as reported in [4, 37] for uncorrelated and long-range correlated disorder distributions.

We now introduce short-range correlated disorder in the frequencies ϵ_i of the CCA (diagonal disorder) based on the random dimer model [49, 51, 53]. Each cavity can take one of two values: $\epsilon_i = \epsilon_0$ or $\epsilon_i = \epsilon_1$. In a given disordered sample (see scheme in Fig. 1), these values are randomly distributed, with a 1/2 probability that an adjacent pair (dimer) of cavities is assigned the frequency ϵ_1, with ϵ_0 being assigned to a single cavity otherwise. This procedure continues for each subsequent non-correlated site, and so on. Our results are qualitatively independent of the values of ϵ_1, the only restriction being that the effective disorder width $|\epsilon_1 - \epsilon_0|$ must not exceed the typical bandwidth (given by $J \equiv 1$). For convenience, we set $\epsilon_0 = 0$, with $\epsilon_1 = 0.5$ or $\epsilon_1 = 1$ throughout.

III. RESULTS

A. Localization properties

Before discussing the properties of the atomic decay, it deems convenient to address the localization properties of the random dimer model, embedded in the free-field Hamiltonian alone, $\hat{H}_0$ [Eq. 1]. This will provides us insights about the non-Markovianity of the emission against the correlated disorder later. For this, we carry out exact numerical diagonalizations over an ensemble of $\hat{H}_0$ to obtain the eigenstates $|\phi_k\rangle = \sum_i c_{k,i}|i\rangle$ alongside their corresponding eigenvalues E_k. The components $c_{k,i}$ represent the individual elements of the mode k at the i-th cavity.

The localization properties will be quantified through the function

$$Z_k^{(A)} = \frac{\left(\sum_{i=1}^{N} |c_{k,i}|^{A/2}\right)^2}{\sum_{i=1}^{N} |c_{k,i}|^{A}}, \tag{8}$$

which accounts for the relative magnitudes and the spatial distribution of the components $c_{k,i}$ throughout the CCA. Depending on the value of A, the function behaves differently: (i) for large values of A, $Z_k^{(A)}$ will be dominated by the largest values of $|c_{k,i}|$, reflecting the fact that those components contribute to more significantly to the eigenstate; (ii) small values of A imply that the contributions from smaller $|c_{k,i}|$ become more balanced and the function $Z_k^{(A)}$ less sensitive to outliers. Also, note that $Z_k^{(A)}$ depends on N. As it increases, the number of components contributing to the sum grows, affecting the outcome. For a strongly localized eigenstate, where the components are concentrated in a small number of $|i\rangle$, the sums in Eq. (8) may not grow significantly with N. In contrast, for a delocalized wavefunction $Z_k^{(A)}$ will grow linearly with N. As a rule of thumb, larger (smaller) values of $Z_k^{(A)}/N$ indicate more (less) localized states.

Figure 2 displays the results for the averaged function $\langle Z^{(A)}\rangle$ versus the eigenvalues E considering $A = 1.5$ and defect frequencies $\epsilon_1 = 1/2$ and $\epsilon_1 = 1$, which will be used henceforth. For each disorder realization, the numerical procedure involves selecting eigenstates whose frequencies fall within a narrow interval centered around E and defining the average $\langle Z^{(A)}\rangle$ over that interval. The quantity is further averaged over the ensemble of disorder realizations and scaled by N, as shown in Fig. 2. Note that the function becomes larger and of N at the resonance point $E = \epsilon_1$, meaning that extended states are to be found around

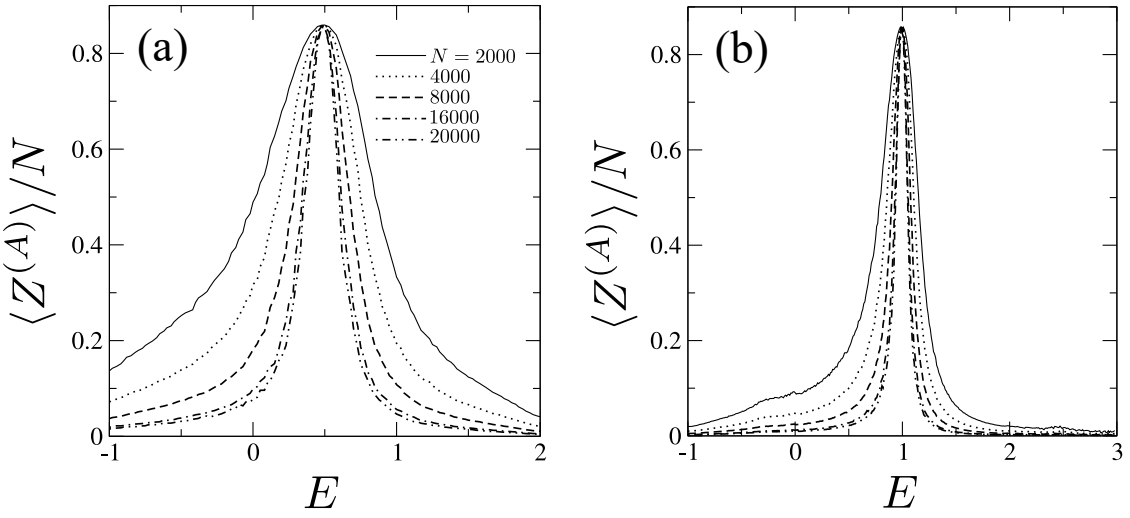

FIG. 2. Localization-measure function $\langle Z^{(A)} \rangle / N$ plotted as a function of the normal mode frequency E for different system sizes N, $A = 1.5$, and considering (a) $\epsilon_1 = 1/2$ and (b) $\epsilon_1 = 1$. All the curves are represent the function averaged over 100 independent realizations of the random-dimer disorder. The results show that $\langle Z^{(A)} \rangle / N$ becomes large and independent of N at $E = \epsilon_1$ that corresponds to the resonances supported by random-dimer disorder configuration, indicating the presence of delocalized states.

that region, as predicted [49, 53]. These resonance regions become narrower for large ϵ_1, this parameter effectively establishing the degree of the disorder.

B. Emission dynamics

We now turn our attention to the relationship between the non-Markovianity of the atomic emission and the transport properties of the random dimer model with respect to the full CCA Hamiltonian $\hat{H} = \hat{H}_0 + \hat{H}_I$. Although a universal definition of quantum non-Markovianity remains elusive, several witnesses and metrics have been proposed typically based on trace distances, divisibility criterion, volume of dynamically accessible states, quantum coherence, and so forth [54–58]. The choice of criterion is often made based on the kind of dissipation channel the system is going through. In our case, considering the initial state $|\psi(0)\rangle = |e\rangle|\text{vac}\rangle$, the reduced density matrix for the atomic state is given by $\rho_e(t) = \text{Tr}_{\text{field}}\{|\psi(t)\rangle\langle\psi(t)|\} = \text{diag}(r(t), 1 - r(t))$, with $r(t) = |f_e(t)|^2$ being the atomic occupation probability. That is, the atom is going through an amplitude damping channel.

Note that we are implicitly assuming $T = 0K$.

The non-Markovianity quantifier we will use is based upon a geometrical description of the volume of accessible states [56]. In our case, this translates into tracking the positive slopes of the square of the return probability, $\partial_t r(t)$, given the it can never increase in the case of Markovian dynamics, $r^2(t)$ being the effective volume. A proper normalized quantifier can be defined as [4]:

$$\mathcal{N} = \frac{\int_{\partial_t r(t)>0} \frac{dr^2(t)}{dt} dt}{|\int_{\partial_t r(t)<0} \frac{dr^2(t)}{dt} dt|}. \tag{9}$$

Note that the denominator tracks the negative slopes instead. This is to prevent divergence of the numerator in the case of persistent oscillations of $r(t)$.

If the atom decays monotonically, then $\mathcal{N} = 0$, indicating full Markovian dynamics. In contrast, undamped Rabi oscillations yield $\mathcal{N} = 1$, representing the maximum non-Markovianity. Note that this case would correspond to an atom interacting with a single field mode, which can be envisaged in the case of extreme disorder, i.e., the spectral density $G(E)$ shares some resemblance to that of a high-Q cavity, possessing an extremely narrow lineshape. Note, however, that the typical $G(E)$ of a high-Q cavity, e.g. a Lorentzian, does not have a cutoff. Hence, in the long-time limit the atom population will be fully found in the lower state. In disordered systems, as in photonic band-gap materials, the atom still decay but a fraction of the population remains trapped [37] due to the non-trivial form of $G(E)$ featuring gaps [14]. Trapping also occurs in homogenous chains due to the formation of bound states inside the structured continuum [33, 34]. We mention that the occurrence of a oscillating steady state accompanying the decay is associated to a certain non-Markovian complexity class with respect to quantum-to-classical transition [24]. It is true, however, that the lattice that interacts the atom also have losses on its own but this is taken as a secondary source of dissipation in most studies.

As we are about to see, the character of the non-Markovianity $\mathcal{N}$ provided by the CCA featuring short-range correlated disorder is governed to the localization strength of the modes more resonant with the atom. These modes effectively define the width of the lineshape around the atomic frequency. To evaluate $\mathcal{N}$, we run the unitary dynamics of the whole (atom plus CCA bath) system tracking the slopes of $r^2(t)$ in each realization of the disorder. We are interested in the dynamics in the long-time regime, with the CCA set large enough so as to avoid field excitation at the boundaries. To achieve this, we numerically evaluate

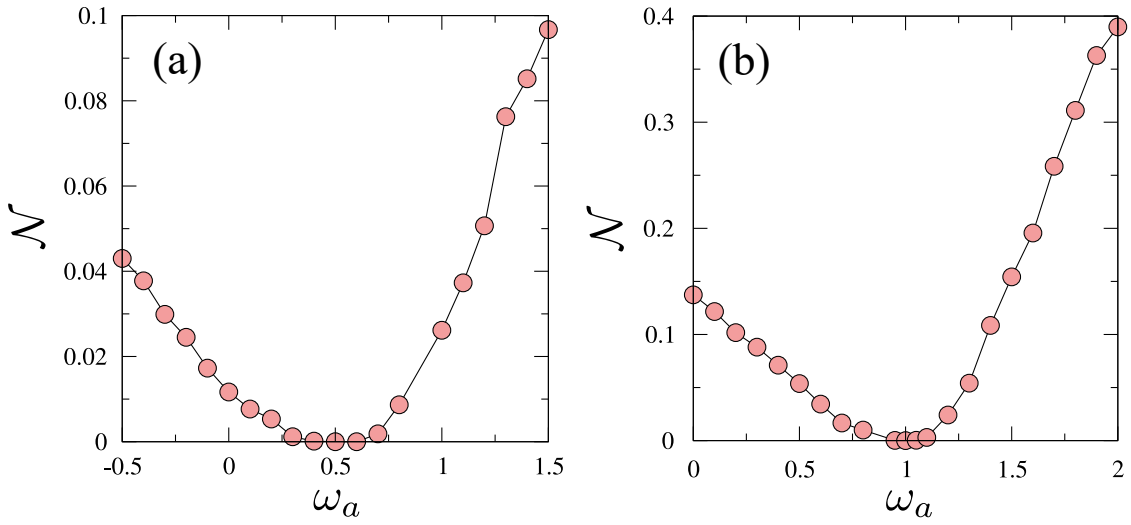

FIG. 3. Non-Markovianity measure $\mathcal{N}$ as a function of the atomic frequency ω_a for (a) $\epsilon_1 = 1/2$ and (b) $\epsilon_1 = 1$. System size is $N = 14001$ and the maximum evolution time is $t \sim 10^3$, assuring no reflections at the boundaries of the CCA. The results are averaged over 100 independent realizations of the random-dimer disorder.

$|\psi(t)\rangle$ by performing a high-order Taylor expansion for the evolution operator

$$\hat{U}(\Delta t) = e^{-i\hat{H}\Delta t} \approx 1 + \sum_{l=1}^{l_o} \frac{(-i\hat{H}\Delta t)^l}{l!}, \tag{10}$$

where l_o is the truncation order. We will set $l_o = 10$ and $\Delta t = 0.1$. The evaluation of high powers of $\hat{H}$ acting on the initial state is be obtained through a recursive formalism described in Ref. [59]. This approach ensures norm conservation over extended time intervals, making it robust for analyzing the desired asymptotic time evolution in large CCAs.

The results for the averaged non-Markovianity measure $\mathcal{N}$ are shown in Fig. 3 as a function of the atomic frequency ω_a. We observe that $\mathcal{N}$ drops to nearly zero as ω_a crosses the frequency corresponding to the dimerized defects, ϵ_1. This behavior highlights a transition between partial non-Markovian behavior to Markovian transition as soon as ω_a becomes resonant with the frequency that support extended states in the random dimer model. Recall that we set $g = 0.1$, which has been shown to be sufficient for the atom to sense the CCA environment as possessing a flat spectral density in the vicinity of ϵ_1. Additionally, the asymmetrical profile of $\mathcal{N}$ can be conceived through close inspection of Fig. 2. The fact that $\mathcal{N}$ is sensitive to subtle changes in the localization strength of the modes is remarkable, even for $\epsilon_1 = 1/2$ [Fig. 3(a)], where the values of $\mathcal{N}$ are typically lower.

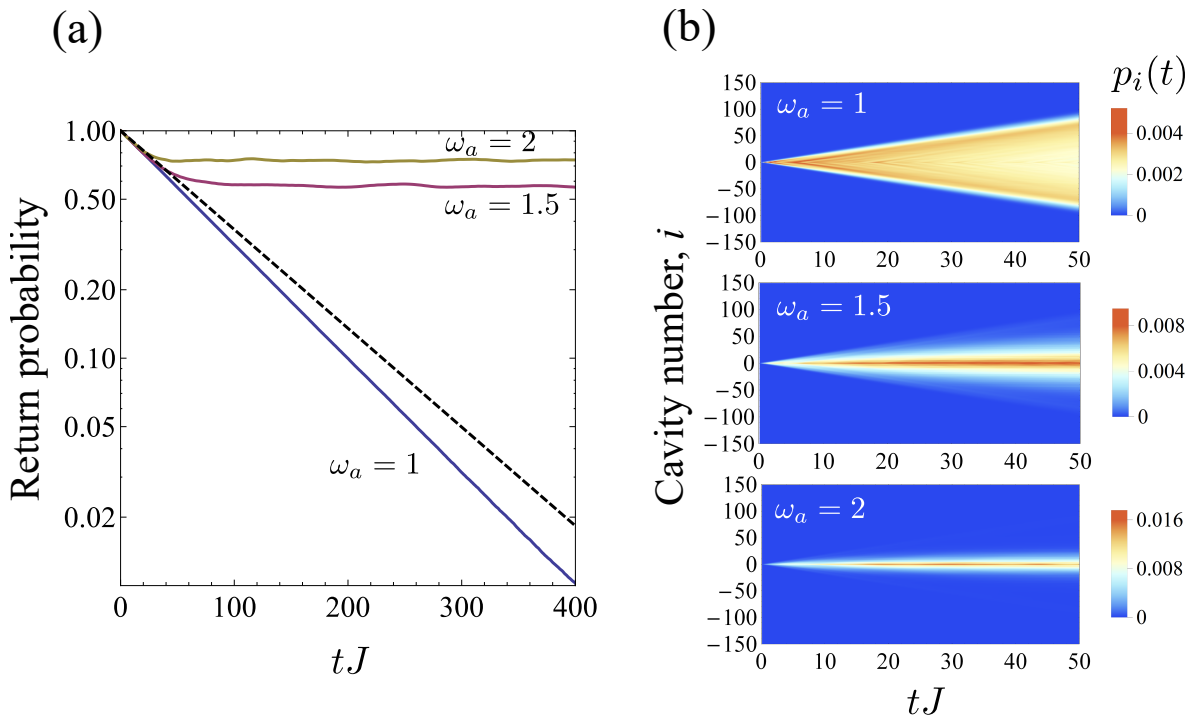

FIG. 4. (a) Return probability $r(t)$ (in log-linear scale) of the atomic excitation versus time for distinct atomic frequencies ω_a, with fixed parameters $\epsilon_1 = 1$, $N = 14001$, and $g = 0.1$. The dashed line is given by $r(t) = e^{-g^2 t/J}$, which represents the decay dynamics in a homogeneous CCA [34]. (b) Corresponding photon dynamics along the CCA given by the local mode probability amplitude $p_i(t) = |\left(\langle g|\langle \mathrm{vac}|\hat{a}_i\right)|\psi(t)\rangle|^2$. All plotted quantities are averaged over 500 independent realizations of the random dimer disorder.

Earlier we mentioned that the atomic excitation undergoes partial trapping in the presence of disorder. Here, this effect should become more pronounced as ω_a moves away from the Markovian resonance point ϵ_1. To confirm this, Fig. 4(a) shows the averaged return probability $r(t)$ for selected values of the atomic frequency ω_a and $\epsilon_1 = 1$ [cf. Fig. 3(b)]. We see that when $\omega_a = \epsilon_1$ the decay indeed follows an exponential function (displayed as a straight line in log-lin scale). The decay corresponding to the homogeneous CCA, $r(t) = e^{-g^2 t/J}$ (with $g = 0.1J$) [34], is also plotted (dashed line) for comparison. As $\omega_a \neq \epsilon_1$ the trapping takes place after an initial transient decay. Intuitively, we expect that the photon becomes localized in a finite region surrounding the emitter in response. For the sake of argument, we show in Fig. 4(b) the corresponding photon propagation dynamics away from the central cavity, given by the local probabilities $p_i(t) = |\left(\langle g|\langle \mathrm{vac}|\hat{a}_i\right)|\psi(t)\rangle|^2$. In the

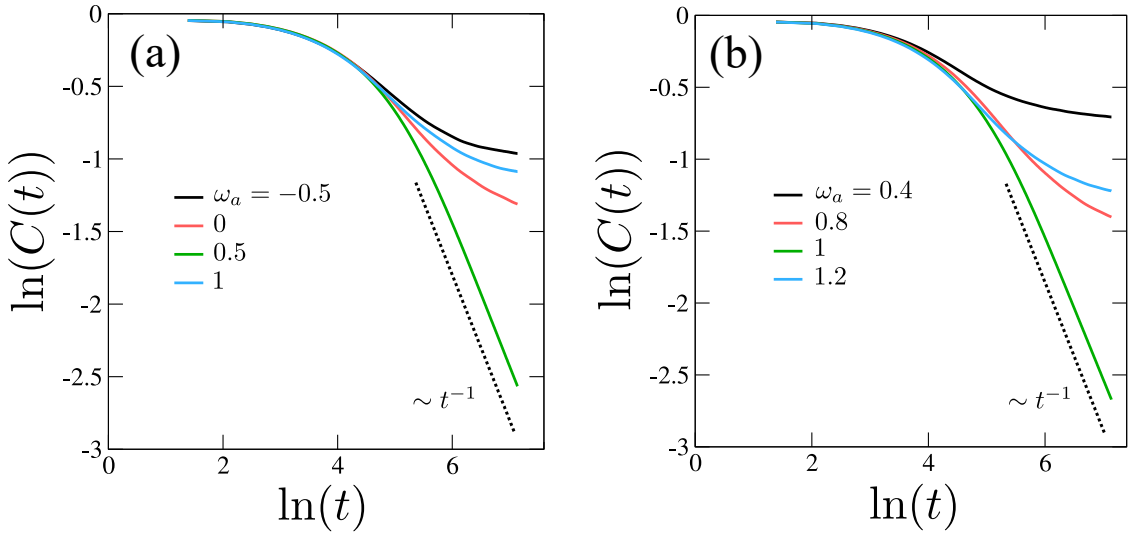

FIG. 5. Logarithm of the autocorrelation function $C(t)$ versus $\ln(t)$ for (a) $\epsilon_1 = 1/2$ and (b) $\epsilon_1 = 1$, with $N = 14001$ and $g = 0.1$. Various atomic frequencies ω_a are considered and the curves represent the average over 100 realizations of the disorder. The slope $\sim t^{-1}$ is included for guiding the eye. This corresponds to the asymptotic limit of $C(t)$ when $\omega_a = \epsilon_1$.

Markovian regime [top panel of Fig. 4(b)], the exponential decay of the atom is followed by ballistic dispersion of the photon through the CCA. Partial photon localization is seen for $\omega_a = 1.5$ (middle panel), where a relatively significant portion of the wavefunction still propagates. Strong localization is observed for $\omega_a = 2$ (bottom panel), which corresponds to $\mathcal{N} \approx 0.4$ (cf. Fig. 3).

Finally, we take a complementary point of view to track the memory effects at play during the atomic emission. Let us define the autocorrelation function:

$$C(t) = \frac{1}{t}\int_0^t r(\tau)d\tau, \tag{11}$$

which effectively characterizes the information flow into the environment. Slow dynamics for $C(t)$ generally indicate the trapping of the atomic excitation around the initial site. If $C(t)$ converges to $1/t$ in the long-time regime, this implies that the atom releases its amplitude to the point where the wave packet state becomes evenly distributed across the array. This latter behavior is a fingerprint of Markovian dynamics. In Fig. 5 we show $\ln(C(t))$ versus $\ln(t)$ for different values of ω_a, again considering $\epsilon_1 = 1/2$ and $\epsilon_1 = 1$. As suggested and evidenced by the linear slopes in both plots, $C(t)$ indeed assumes $\sim 1/t$ asymptotically when $\omega_a = \epsilon_1$ (cf. Fig. 3). Otherwise, the decay is slower than $1/t$, amounting to partial trapping

of the atomic excitation and thereby some degree of non-Markovianity.

IV. CONCLUSIONS

A single two-level atom interacting with structured environments inspired by low-dimensional condensed-matter models exhibits rich dynamics. In this study, we explored the interplay between short-range correlated disorder and non-Markovianity in the process of spontaneous emission of a two-level atom into a CCA. The disorder was introduced in the form of dimerized defects [49] with frequency ϵ_1. We found that when the atomic frequency ω_a is in resonance with ϵ_1, the atom undergoes Markovian (memoryless) exponential decay due to the contribution of delocalized field modes, entailing an effective flat spectral density [4]. In contrast, when ω_a deviates from resonance, the amplitude damping channel retains memory, leading to information backflow originating from the partial localization of the photon. Here, the degree of non-Markovianity was captured by the quantity $\mathcal{N}$, rooted on change of the volume of accessible physical states [56]. We stress that there are many other non-Markovian criteria in the literature [54, 55, 57] and relying on just one may be misleading. However, in view of the type of amplitude channel considered in this work, $\rho_e(t) = \mathrm{diag}(r(t), 1-r(t))$, non-Markovianity was manifested whenever the slope of $r(t)$ was positive [4, 37]. Another quantifier that falls into the same class is the one introduced in Ref. [55], which relies on the evolution of entanglement between the system of interest and an ancilla protected from the bath. Non-Markovianity in this case is detected by any increase in the bipartite entanglement over time and quantified accordingly. This arises because the local action of complete positive trace-preserving maps cannot increase entanglement and therefore the Markovian regime is characterized by a monotonic decay. A complementary tool, namely the autocorrelation funcion $C(t)$, was employed here instead as a dynamical measure of the memory effects.

By studying the interplay between the transport properties of low-dimensional systems and information flow we seek to provide tools for tailored quantum dissipation, hence contributing to the design of, e.g,. analog simulators of open quantum systems [9, 11]. Furthermore, the atom (or any other small subset a larger system) could act as a probe of many-body properties [4, 43–46]. Here, the resonance between the frequencies ω_a and ϵ_1 acted as the control parameter for non-Markovianity and localization. We mention that

random-dimer chains can be manufactured in state-of-the-art photonics [51, 52] and thus experimental realization of our findings could be sought by proper interfacing with a qubit [60].

ACKNOWLEDGEMENTS

This work was supported by FAPEAL (Alagoas State agency), CAPES, and CNPq (Federal agencies).

---

[1] J. Preskill, Quantum computing and the entanglement frontier, (2012), arXiv:1203.5813 [quant-ph].

[2] H.-P. Breuer, E.-M. Laine, J. Piilo, and B. Vacchini, Colloquium: Non-markovian dynamics in open quantum systems, Rev. Mod. Phys. **88**, 021002 (2016).

[3] C. J. Myatt, B. E. King, Q. A. Turchette, C. A. Sackett, D. Kielpinski, W. M. Itano, C. Monroe, and D. J. Wineland, Decoherence of quantum superpositions through coupling to engineered reservoirs, Nature **403**, https://doi.org/10.1038/35002001 (2000).

[4] S. Lorenzo, F. Lombardo, F. Ciccarello, and G. M. Palma, Quantum non-markovianity induced by anderson localization, Sci. Rep. 7 **42729**, 10.1038/srep42729 (2017).

[5] D. F. Urrego, J. Flórez, J. c. v. Svozilík, M. Nuñez, and A. Valencia, Controlling non-markovian dynamics using a light-based structured environment, Phys. Rev. A **98**, 053862 (2018).

[6] V. S. Ferreira, J. Banker, A. Sipahigil, M. H. Matheny, A. J. Keller, E. Kim, M. Mirhosseini, and O. Painter, Collapse and revival of an artificial atom coupled to a structured photonic reservoir, Phys. Rev. X **11**, 041043 (2021).

[7] A. González-Tudela and J. I. Cirac, Quantum emitters in two-dimensional structured reservoirs in the nonperturbative regime, Phys. Rev. Lett. **119**, 143602 (2017).

[8] J. Lira and L. Sanz, Schrödinger cats coupled with cavities losses: the effect of finite and structured reservoirs, J. Opt. Soc. Am. B **41**, C254 (2024).

[9] C. W. Kim, J. M. Nichol, A. N. Jordan, and I. Franco, Analog quantum simulation of the dynamics of open quantum systems with quantum dots and microelectronic circuits, PRX Quantum **3**, 040308 (2022).

[10] X. Li, S.-X. Lyu, Y. Wang, R.-X. Xu, X. Zheng, and Y. Yan, Toward quantum simulation of non-markovian open quantum dynamics: A universal and compact theory, Phys. Rev. A **110**, 032620 (2024).

[11] C. Gaikwad, D. Kowsari, C. Brame, X. Song, H. Zhang, M. Esposito, A. Ranadive, G. Cappelli, N. Roch, E. M. Levenson-Falk, and K. W. Murch, Entanglement assisted probe of the non-markovian to markovian transition in open quantum system dynamics, Phys. Rev. Lett. **132**, 200401 (2024).

[12] F. Verstraete, M. M. Wolf, and J. Ignacio Cirac, Quantum computation and quantum-state engineering driven by dissipation, Nature Physics **5**, https://doi.org/10.1038/nphys1342 (2009).

[13] M. E. J. M. K. W. Harrington, Patrick M., Engineered dissipation for quantum information science, Nature Reviews Physics **4**, https://doi.org/10.1038/s42254-022-00494-8 (2022).

[14] P. Lambropoulos, G. M. Nikolopoulos, T. R. Nielsen, and S. Bay, Fundamental quantum optics in structured reservoirs, Reports on Progress in Physics **63**, 455 (2000).

[15] H. Breuer and F. Petruccione, *The Theory of Open Quantum Systems* (Clarendon, 2002).

[16] D. G. Angelakis, P. L. Knight, and E. Paspalakis, Photonic crystals and inhibition of spontaneous emission: an introduction, Contemporary Physics **45**, 303 (2004), https://doi.org/10.1080/00107510410001676795.

[17] L. Sapienza, H. Thyrrestrup, S. Stobbe, P. D. Garcia, S. Smolka, and P. Lodahl, Cavity quantum electrodynamics with anderson-localized modes, Science **327**, 1352 (2010).

[18] A. D. Dente, R. A. Bustos-Marún, and H. M. Pastawski, Dynamical regimes of a quantum swap gate beyond the fermi golden rule, Phys. Rev. A **78**, 062116 (2008).

[19] B.-H. Liu, L. Li, Y.-F. Huang, C.-F. Li, G.-C. Guo, E.-M. Laine, H.-P. Breuer, and J. Piilo, Experimental control of the transition from markovian to non-markovian dynamics of open quantum systems, Nature Physics **7**, 931 (2011).

[20] T. J. G. Apollaro, C. Di Franco, F. Plastina, and M. Paternostro, Memory-keeping effects and forgetfulness in the dynamics of a qubit coupled to a spin chain, Phys. Rev. A **83**, 032103 (2011).

[21] K. H. Madsen, S. Ates, T. Lund-Hansen, A. Löffler, S. Reitzenstein, A. Forchel, and P. Lodahl, Observation of non-markovian dynamics of a single quantum dot in a micropillar cavity, Phys. Rev. Lett. **106**, 233601 (2011).

[22] F. Pastawski, L. Clemente, and J. I. Cirac, Quantum memories based on engineered dissipation, Phys. Rev. A **83**, 012304 (2011).

[23] Z.-X. Man, N. B. An, and Y.-J. Xia, Non-markovian dynamics of a two-level system in the presence of hierarchical environments, Opt. Express **23**, 5763 (2015).

[24] H.-N. Xiong, P.-Y. Lo, W.-M. Zhang, D. H. Feng, and F. Nori, Non-markovian complexity in the quantum-to-classical transition, Scientific Reports **5**, 13353 (2015).

[25] Y.-L. L. Fang, F. Ciccarello, and H. U. Baranger, Non-markovian dynamics of a qubit due to single-photon scattering in a waveguide, New Journal of Physics **20**, 043035 (2018).

[26] H. Z. Shen, S. Xu, H. T. Cui, and X. X. Yi, Non-markovian dynamics of a system of two-level atoms coupled to a structured environment, Phys. Rev. A **99**, 032101 (2019).

[27] A. K. Singh, L. Chotorlishvili, S. Srivastava, I. Tralle, Z. Toklikishvili, J. Berakdar, and S. K. Mishra, Generation of coherence in an exactly solvable nonlinear nanomechanical system, Phys. Rev. B **101**, 104311 (2020).

[28] V. E. Tarasov, Non-markovian dynamics of open quantum system with memory, Annals of Physics **434**, 168667 (2021).

[29] M. Kaczor, I. Tralle, P. Jakubczyk, S. Stagraczyński, and L. Chotorlishvili, Switching of the information backflow between a helical spin system and non-markovian bath, Annals of Physics **442**, 168918 (2022).

[30] D. Gribben, A. Strathearn, G. E. Fux, P. Kirton, and B. W. Lovett, Using the Environment to Understand non-Markovian Open Quantum Systems, Quantum **6**, 847 (2022).

[31] G. Mouloudakis, T. Ilias, and P. Lambropoulos, Arbitrary-length xx spin chains boundary-driven by non-markovian environments, Phys. Rev. A **105**, 012429 (2022).

[32] G. Mouloudakis and P. Lambropoulos, Coalescence of non-markovian dissipation, quantum zeno effect, and non-hermitian physics in a simple realistic quantum system, Phys. Rev. A **106**, 053709 (2022).

[33] S. Longhi, Bound states in the continuum in a single-level fano-anderson model, The European Physical Journal B **57**, 45 (2007).

[34] F. Lombardo, F. Ciccarello, and G. M. Palma, Photon localization versus population trapping in a coupled-cavity array, Phys. Rev. A **89**, 10.1103/PhysRevA.89.053826 (2014).

[35] S. Lorenzo, F. Ciccarello, and G. M. Palma, Non-markovian dynamics from band edge effects and static disorder, International Journal of Quantum Information **15**, 1740026 (2017).

[36] F. Cosco and S. Maniscalco, Memory effects in a quasiperiodic fermi lattice, Phys. Rev. A **98**, 053608 (2018).

[37] M. O. Monteiro, N. K. Bernardes, E. M. Broni, F. A. B. F. de Moura, and G. M. A. Almeida, Non-markovian to markovian decay in structured environments with correlated disorder, Phys. Rev. A **111**, 022212 (2025).

[38] J. Preskill, Quantum Computing in the NISQ era and beyond, Quantum **2**, 79 (2018).

[39] H. Lyyra, O. Siltanen, J. Piilo, S. Banerjee, and T. Kuusela, Experimental quantum probing measurements with no knowledge of the system-probe interaction, Phys. Rev. A **102**, 022232 (2020).

[40] D. Tamascelli, C. Benedetti, H.-P. Breuer, and M. G. A. Paris, Quantum probing beyond pure dephasing, New Journal of Physics **22**, 083027 (2020).

[41] S. Blair, G. Zicari, A. Belenchia, A. Ferraro, and M. Paternostro, Nonequilibrium quantum probing through linear response, Phys. Rev. Res. **6**, 013152 (2024).

[42] J. Barr, G. Zicari, A. Ferraro, and M. Paternostro, Spectral density classification for environment spectroscopy, Machine Learning: Science and Technology **5**, 015043 (2024).

[43] M. Gessner, M. Ramm, H. Häffner, A. Buchleitner, and H.-P. Breuer, Observing a quantum phase transition by measuring a single spin, Europhysics Letters **107**, 40005 (2014).

[44] Y.-C. Lin, P.-Y. Yang, and W.-M. Zhang, Non-equilibrium quantum phase transition via entanglement decoherence dynamics, Scientific Reports **6**, 34804 (2016).

[45] G. L. Giorgi, S. Longhi, A. Cabot, and R. Zambrini, Quantum probing topological phase transitions by non-markovianity, Annalen der Physik **531**, 1900307 (2019).

[46] D. Rossini and E. Vicari, Coherent and dissipative dynamics at quantum phase transitions, Physics Reports **936**, 1 (2021), coherent and dissipative dynamics at quantum phase transitions.

[47] P. W. Anderson, Absence of diffusion in certain random lattices, Phys. Rev. **109**, 1492 (1958).

[48] F. Izrailev, A. Krokhin, and N. Makarov, Anomalous localization in low-dimensional systems with correlated disorder, Physics Reports **512**, 125 (2012).

[49] D. H. Dunlap, H.-L. Wu, and P. W. Phillips, Absence of localization in a random-dimer model, Phys. Rev. Lett. **65**, 88 (1990).

[50] V. Bellani, E. Diez, R. Hey, L. Toni, L. Tarricone, G. B. Parravicini, F. Domínguez-Adame, and R. Gómez-Alcalá, Experimental evidence of delocalized states in random dimer superlattices,

Phys. Rev. Lett. **82**, 2159 (1999).

[51] U. Naether, S. Stützer, R. A. Vicencio, M. I. Molina, A. Tünnermann, S. Nolte, T. Kottos, D. N. Christodoulides, and A. Szameit, Experimental observation of superdiffusive transport in random dimer lattices, New Journal of Physics **15**, 013045 (2013).

[52] Z.-S. Xu, J. Gao, A. Iovan, I. M. Khaymovich, V. Zwiller, and A. W. Elshaari, Observation of reentrant metal-insulator transition in a random-dimer disordered ssh lattice, npj Nanophotonics **1**, 8 (2024).

[53] G. M. A. Almeida, M. L. Lyra, and F. A. B. F. de Moura, Transmission of quantum states through disordered channels with dimerized defects, Quantum Information Processing **18**, 350 (2019).

[54] H.-P. Breuer, E.-M. Laine, and J. Piilo, Measure for the degree of non-markovian behavior of quantum processes in open systems, Physical Review Letters **103**, 210401 (2009).

[55] A. Rivas, S. F. Huelga, and M. B. Plenio, Entanglement and non-markovianity of quantum evolutions, Physical Review Letters **105**, 050403 (2010).

[56] S. Lorenzo, F. Plastina, and M. Paternostro, Geometrical characterization of non-markovianity, Phys. Rev. A **88**, 020102 (2013).

[57] Ángel Rivas, S. F. Huelga, and M. B. Plenio, Quantum non-markovianity: characterization, quantification and detection, Reports on Progress in Physics **77**, 094001 (2014).

[58] T. Chanda and S. Bhattacharya, Delineating incoherent non-markovian dynamics using quantum coherence, Annals of Physics **366**, 1 (2016).

[59] F. A. B. F. de Moura, Dynamics of One-Electron in a One-Dimensional Systems with AN Aperiodic Hopping Distribution, International Journal of Modern Physics C **22**, 63 (2011).

[60] E. Kim, X. Zhang, V. S. Ferreira, J. Banker, J. K. Iverson, A. Sipahigil, M. Bello, A. González-Tudela, M. Mirhosseini, and O. Painter, Quantum electrodynamics in a topological waveguide, Phys. Rev. X **11**, 011015 (2021).